Available online at www.sciencedirect.com

Journal of Photochemistry and Photobiology A: Chemistry 178 (2006) 251–257

Journal of Photochemistry and Photobiology A:Chemistry

www.elsevier.com/locate/jphotochem

Emission properties of a highly fluorescent pyrene dye in solution and in the liquid state

Véronique de Halleux [a], Wael Mamdouh [b], Steven De Feyter [b,*], Frans De Schryver [b], Jérémy Levin [a], Yves Henri Geerts [a,**]

[a] *Laboratoire de Chimie des Polymères, Université Libre de Bruxelles CP 206/01, Bld du Triomphe, 1050 Bruxelles, Belgium*
[b] *Department of Chemistry, Molecular and Nano Materials, Laboratory of Photochemistry and Spectroscopy,*
Katholieke Universiteit Leuven, Celestijnenlaan 200 F, B-3001 Leuven, Belgium

---

Abstract

Three novel pyrene dyes substituted by four oligo-ether side chains of varying size have been synthesized. Surprisingly, two of these fluorescent derivatives are liquid at room temperature. The photophysical study of one of these dyes, which is miscible in common organic solvents such as hexane, chloroform and toluene, but also in water, has been performed. It has been shown that this pyrene derivative exhibits a high quantum yield of fluorescence, $\Phi_f \sim 1$, and has a high extinction coefficient, i.e. $\varepsilon = 100{,}000\,\mathrm{mol^{-1}\,cm^{-1}\,l}$, in diluted *n*-hexane solution. In water, aggregation takes place and the fluorescence quantum yield decreases considerably. Moreover, the spectroscopic properties of the aggregates formed in water are very close to those of the neat liquid. Therefore, the basic structure of the aggregates formed in water and in the pure liquid are expected to be similar.

Keywords: Liquid; Supramolecular chemistry; Aggregation; Fluorescence; Pyrene

---

1. Introduction

Since several decades, there has been a wide utilisation of fluorescent molecular probes for various purposes [1]. Examples are numerous: the investigation of macromolecular conformations [2], the microenvironments of organized media, such as micelles [3], LB films [4] and bilayers [5], the DNA duplex formation between complementary oligonucleotides [6] and the mechanism for binding RNA to a ribozyme [7], metal cation detection [8] and molecular-recognition process [9]. Amongst the fluorescent probes, pyrene and perylene derivatives are rather attractive because they exhibit generally a rather high quantum yield of fluorescence (Φ_f) in dilute solution combined with high photostability [10,11]. Φ_f tends to drop when going from good to poor solvents, such as water [12]. This decrease results to a large extent from aggregation that causes interactions between π-systems in ground and excited states [13,14]. Ground state aggregation of water-soluble perylene derivatives has been investigated in great details by a combined small angle neutron scattering, proton NMR spectroscopy and UV–vis spectroscopy. [15] Anticooperative association process, i.e. dimerisation favoured over oligomerisation, has been demonstrated [15]. However, the decrease of Φ_f has not been reported. Other perylene derivatives with Φ_f as high as 0.66 in water have been reported by Müllen and co-workers [12]. These water-soluble fluorescent dyes have also been used in cardiac cell culture [12]. Water-soluble pyrene derivatives have been investigated too. For example, a quantitative treatment of 4-(1-pyrene)butanoate aggregation properties in aqueous environment has recently been reported [16]. Conclusions were that this pyrene derivative has not only a significant propensity for aggregation in the excited state but also in the ground state. Encouraged by these recent results and motivated by the wish to understand the role of molecular and supramolecular structure on the fluorescence of neutral π-systems in lyotropic and thermotropic mesophases, we embarked on the synthesis and study of three novel pyrene derivatives: 1,3,6,8-tetrakis(4-*n*-monoethyleneglycol-(2-propynyl)ether)pyrene (**6a**), 1,3,6,8-tetrakis(4-*n*-diethyleneglycol-(2-propynyl)ether)pyrene (**6b**) and 1,3,6,8-tetrakis(4-*n*-triethyleneglycol-(2-propynyl)ether)pyre-

---

[*] Corresponding author. Tel.: +32 1 632 79 21; fax: +32 1 632 79 90.
[**] Corresponding author. Tel.: +32 2 650 53 90; fax: +32 2 650 54 10.
E-mail addresses: Steven.Defeyter@chem.kuleuven.be (S. De Feyter), ygeerts@ulb.ac.be (Y.H. Geerts).

1010-6030/$ – see front matter © 2005 Elsevier B.V. All rights reserved.
doi:10.1016/j.jphotochem.2005.10.039

ne (**6c**). **6b** is a liquid at room temperature and has been chosen for further investigations. A comprehensive spectroscopic study as a function of concentration and solvent indicates ground-state aggregation.

2. Experimental/materials and methods

2.1. Reagents, catalysts and solvents

Toluene (Aldrich, A.C.S. reagent) was refluxed over calcium chloride and freshly distilled before use. Triethylamine was dried over sodium hydroxide and freshly distilled before use. Tetrahydrofuran was used as received from Aldrich as A.C.S. reagent. Sodium hydride (80% dispersion in oil), triethyleneglycol monoethylether (95+%), diethyleneglycol monoethylether (95+%), monoethyleneglycol monoethylether propylbromide (95+%), propargylbromide (80 wt.% solution in toluene), nitrobenzene, pyrene, bromine, tetrakis(triphenylphosphine)–palladium (0) and copper iodide, were used as commercially available grade from Aldrich. *n*-Hexane was of spectroscopic grade (98–99%). The ultrapure water (Milli-Q) was obtained by using a filter system with several filtration steps (Millipore, Cat. no. CFOF 012 05) to remove ions, organic materials and small particles. The resistivity was 18 MΩ.

2.2. General methods

The mesomorphic behaviour of **6a–c** was investigated by polarizing optical microscopy (Aus JENA microscope equipped with a Mettler FP 52 hot stage) and by differential scanning calorimetry (Mettler Toledo DSC 821 and 3 mg sample in closed Al pans) with heating and cooling scans performed at 10 °C min^{-1} (peak values are given).

^{1}H NMR (250 and 300 MHz) and ^{13}C (75 MHz) spectra were recorded on a Bruker AMX 3000 and Bruker DRX 500 and 600 spectrometer. $CDCl_3$ was used as a solvent and the solvent signal was used as internal standard. Chemical shifts are reported as δ (ppm). Mass spectra were recorded on an Intectra GmbH, AMD 402 instrument (electron impact, 70 eV).

2.2.1. Absorption spectroscopy

Absorption spectra were recorded with a double-beam UV–vis spectrophotometer (Perkin-Elmer Instruments, series Lambda40). For the solution experiments, cells with a 1 cm, 1 mm or 0.1 mm path length, the latter one realized by a 1 mm cell with a 0.9 mm quartz spacer, were used depending on the concentration of the solution. Absorption spectra of oily **6b** were recorded on a quartz slide.

2.2.2. Steady-state fluorescence spectroscopy

Steady-state fluorescence spectra were recorded with a fluorimeter (Spex fluorolog, model 1691). Diluted solutions were measured in cells with 1 cm path length in the right angle mode. More concentrated solutions, measured in 1 mm or 0.1 mm cells, and a film of oily **6b** on a quartz plate, were measured in the front face configuration. The latter means that the angle between the excitation light and the detected fluorescence light is 26°, while for the right angle configuration this angle equals 90°. Generally, the sample was perpendicular to the incoming light beam. The emission spectra were corrected for fluctuations of the lamp intensity as well as the wavelength dependency of the photo multiplier tube detector (PMT). The reference method was used to determine the quantum yield of fluorescence. The fluorescence quantum yield of **6b** in *n*-hexane has been determined with perylene in toluene as a reference. The fluorescence quantum yield of **6b** in water has been determined with Rhodamine 6G in ethanol and fluoresceine in 0.1 M sodium hydroxide as a Ref. [17].

2.2.3. Time-resolved fluorescence spectroscopy

Fluorescence decays have been obtained via the ‘single photon counting’ technique [18]. The samples were excited at 377 nm by the frequency doubled output of a regeneratively mode-locked Ti:sapphire laser Ti:Sa (Tsunami model 3950D, Spectra Physics), pumped by all visible lines of a continuous wave argon ion laser Ar^+ (BeamLock model 2028A-12, Spectra Physics). Suitable filters were placed in the detection path to suppress remaining excitation light. The diameter of the beam was 1–2 mm, where the width of the instrument response function (IRF) was 38 ps and the time increment for all samples was 3.52 ps. The decays were fitted and analyzed using the least-squares (LS) method and the decays for the excited species were analyzed by linking the instrument response function, scatter over all the recorded decay traces within the decay run. The quality of the fits has been judged from the values of the reduced χ^2 as well as from the residuals and the autocorrelation function.

2.3. Synthesis

Mono-di and tri-ethyleneglycol-2-propynylether (**3a–c**) (Scheme 1) were synthesized following a literature procedure [19]. Tetrabromopyrene **5** was obtained by the procedure of Volmmann et al. [20].

2.3.1. 1,3,6,8-tetrakis(4-n-diethyleneglycol-(2-propynyl)ether)pyrene (*6b*)

3b (1.26 g, 8 mmol and 8 equiv.), **5** (0.518 g and 1 mmol), $Pd(PPh_3)_4$ (92 mg, 0.09 mmol and 8 mol%) and copper iodine (19 mg, 0.1 mmol and 10 mol%) were added to a mixture of toluene and triethylamine (50:50 mL). The reaction mixture was stirred, under nitrogen, at 80 °C for 24 h. Then it was poured into a solution of ice and concentrated hydrochloric acid (3:1). The organic phase was extracted with dichloromethane, dried over magnesium sulfate and the crude product was purified by column chromatography on silica gel with tetrahydrofuran:toluene (3:4) as eluent to give 87% of **6b** (0.72 g and 0.87 mmol).

^{1}H NMR (300 MHz, $CDCl_3$): $\delta = 8.58$ (s, 4H, CH), 8.25 (s, 2H, CH), 4.65 (s, 8H; CH_2), 3.92 (m, 8H; CH_2), 3.78 (m, 8H; CH_2), 3.71 (m, 8H; CH_2), 3.58 (m, 8H; CH_2) and 3.38 (s, 12H; CH_3). ^{13}C NMR (75 MHz, $CDCl_3$): $\delta = 134.28$, 131.96, 126.90, 123.73, 118.25, 91.85, 84.21, 71.96, 70.65, 70.58, 69.43, 59.45 and 59.06. MS: (electro spray): *m*/*z* 849.5 $M + Na^+$, 100%, calculated 849.38; *m*/*z* 865.5 $M + K^+$, 40%, calculated 865.48.

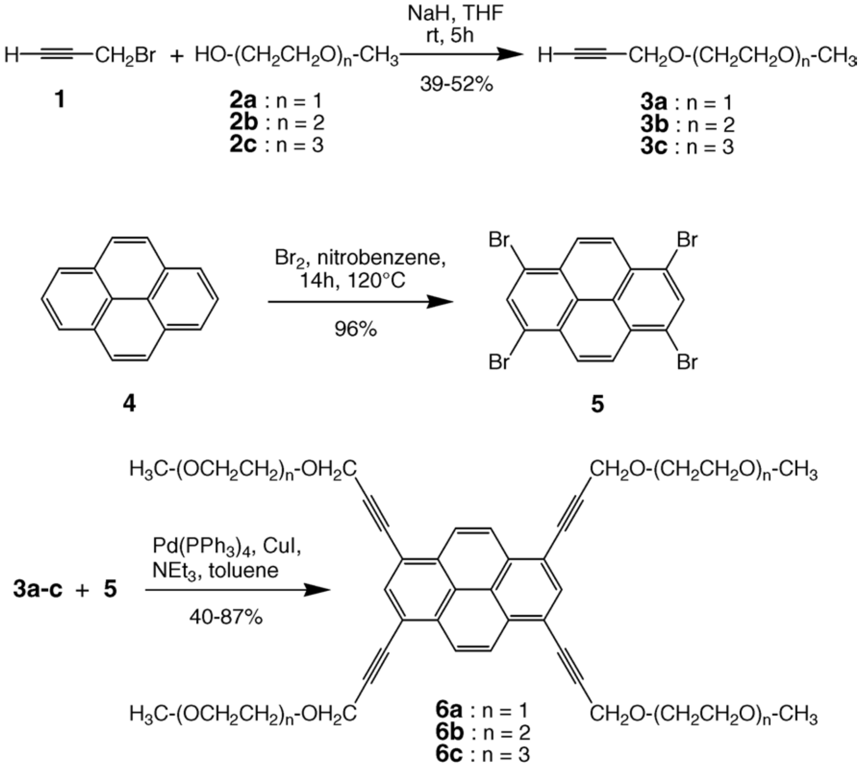

Scheme 1. Synthetic pathway to pyrene derivatives **6a–c**.

UV–vis (absorption in *n*-hexane) $\lambda_{max} = 422$ nm and (emission in *n*-hexane) $\lambda_{max} = 425$ nm.

*2.3.2. 1,3,6,8-tetrakis(4-n-triethyleneglycol-(2-propynyl)ether)pyrene (**6c**)*

Compound **6c** was synthesized by the same procedure described for the preparation of **6b**. **3c** (3 g, 15 mmol and 8 equiv.), **5** (0.95 g and 1.82 mmol), $Pd(PPh_3)_4$ (170 mg, 0.146 mmol and 8 mol%) and copper iodine (35 mg, 0.185 mmol and 10 mol%) were added in a mixture of toluene:triethylamine (150:150 mL). After aqueous work-up, the crude product was purified by column chromatography on silica gel with toluene:methanol (8:2) as eluent to give 62% of **6c** (1.13 g and 1.13 mmol).

^{1}H NMR (250 MHz, $CDCl_3$): $\delta = 8.60$ (s, 4H, CH), 8.26 (s, 2H, CH), 4.60 (s, 8H; CH_2), 3.88 (m, 8H; CH_2), 3.76 (m, 8H; CH_2), 3.67 (m, 24H; CH_2), 3.52 (m, 8H; CH_2) and 3.34 (s, 12H; CH_3). ^{13}C NMR (75 MHz, $CDCl_3$): $\delta = 134.28$, 131.95, 126.89, 123.73, 118.23, 91.84, 84.21, 71.95, 70.65, 70.58, 69.42, 59.45 and 59.07. MS: (electro spray): *m/z* 1025.5 $M + Na^+$, 100%, calculated 1025.49; *m/z* 1041.5 $M + K^+$, 80%, calculated 1040.60. UV–vis (absorption in *n*-hexane) $\lambda_{max} = 422$ nm and (emission in *n*-hexane) $\lambda_{max} = 425$ nm.

*2.3.3. 1,3,6,8-tetrakis(4-n-monoethyleneglycol-(2-propynyl)ether)pyrene (**6a**)*

Compound **6a** was synthesized by the same procedure described for the preparation of **6b**. **3a** (0.32 g, 2.8 mmol and 6 equiv.), **5** (0.245 g and 0.47 mmol), $Pd(PPh_3)_4$ (44 mg, 0.059 mmol and 8 mol%) and copper iodine (9 mg, 0.047 mmol and 10 mol%) were reacted in a mixture of toluene:triethylamine (50:50 mL). After aqueous work-up, the crude product was purified by column chromatography on silica gel with ethyl acetate as eluent, followed by recrystallisation in hexane to give 40% of **6a** (0.123 g and 0.19 mmol).

Mp = 63 °C. ^{1}H NMR (250 MHz, $CDCl_3$): $\delta = 8.58$ (s, 4H, CH), 8.25 (s, 2H, CH), 4.66 (s, 8H; CH_2), 3.90 (m, 8H; CH_2), 3.68 (m, 8H; CH_2) and 3.34 (s, 12H; CH_3). ^{13}C NMR (75 MHz, $CDCl_3$): $\delta = 134.24$, 131.95, 126.68, 118.21, 91.73, 84.28, 71.82, 69.26, 59.47 and 59.18. UV–vis (absorption in *n*-hexane) $\lambda_{max} = 422$ nm and (emission in *n*-hexane) $\lambda_{max} = 425$ nm.

3. Results and discussion

3.1. Synthesis

The synthesis of **6a–c** is outlined in Scheme 1. In a first step mono-di and tri-ethyleneglycol-2-propynylether (**3a–c**) were obtained in a 39–52% yield by the nucleophilic substitution of mono-di or tri-ethyleneglycol **2a–c** on propargylbromide (**1**) following a procedure described in literature [19]. In a second step tetrabromopyrene **5** was obtained in a 96% yield by a procedure developed by Volmmann et al. which consists of an electrophilic substitution of bromine on pyrene (**4**) in nitrobenzene [20]. Finally, the alkyne chains **3a–c** were coupled to tetrabromopyrene **5** by the Haghiara–Sonogashira method [21] to give **6a–c** in 40–87% yield depending on the ease of purification.

Table 1
Calorimetric data of compound **6a**, recorded at 10 °C/min

Compound	Process	Temperature (°C)	Enthalpy (kJ/mol)
6a	Heating	31	4.4
		63	20.6
	Cooling	20	−4.3
		33	−20.5

3.2. Thermotropic and lyotropic properties

A columnar thermotropic or lyotropic liquid crystalline phase was expected from the molecular structure of **6a–c** [22–24]. Indeed, **6a–c** are composed of a discotic rigid hydrophobic core surrounded by four flexible polar chains with a clear amphiphilic character. The thermotropic behaviour of **6a** investigated by differential scanning calorimetry (DSC) (Table 1) and polarized optical microscopy (POM) reveal a polymorphism but no mesomorphism. The transition enthalpy of melting is rather low for such a large molecule and indicates the occurrence of a crystalline phase with a weak cohesive energy. This is also corroborated by the low clearing temperature for a molecule containing twenty-four carbon atoms in its rigid conjugated core and an equal number of carbon and oxygen atoms in the flexible side chains.

The lyotropic propensity of **6a–c** in hexane:water solutions was investigated using contact preparations [25]. However, none of the samples showed any birefringence under the optical cross-polarized microscope, even under shearing indicating the absence of lyotropic phase. Beside the absence of liquid crystalline phase, the liquid character of **6b** and **6c** is surprising. However, the liquid character at room temperature and miscibility in non-polar to polar solvents qualify **6b** and **6c** as original candidates to study emissive properties from dilute solution to neat phase without the perturbing effect of phase transition.

3.3. Aggregate formation of **6b** in apolar solvents

Fig. 1a reflects the steady-state absorption and emission spectra of **6b** (∼1 μM) in *n*-hexane. The spectra are characterized by a clear vibronic progression (absorption: 422, 398, and 378 nm and emission: 425, 452 and 484 nm) and a very small Stokes shift. The extinction coefficient at 422 nm is 10^5 mol^{-1} cm^{-1} l. **6b** is highly fluorescent and Φ_f approaches unity.

In contrast to pyrene, the lowest transition are symmetry allowed, which is also reflected by the fluorescence lifetime determined by time-correlated single photon counting ($\tau = 2.65$ ns), which is mono-exponential and much shorter than that for pyrene [26,27] and independent of the emission wavelength. At higher concentrations, the absorption spectra become concentration dependent, characterized by a tail in the bathochromic edge of the absorption spectrum (Fig. 1b). Upon excitation at 410 nm, emission spectra show in addition to the vibronic peaks related to monomer emission, a weak emission band with a maximum at ∼570 nm, which can be attributed to emission of the aggregates (not shown). The excitation spectra (Fig. 1c) show very clearly the effect of aggregation. When the emission is collected at 430 nm, the excitation spectrum reflects the absorption spectrum of the monomer with the characteristic vibronic progression between 350 and 425 nm. At collection of the emission light at 570 nm, which we attribute to aggregate emission, the excitation spectrum is broadened and red shifted and resembles the absorption and excitation spectra in neat liquid (see Fig. 3c and vide infra). These data proves that both monomer and ground-state aggregates are present in solution.

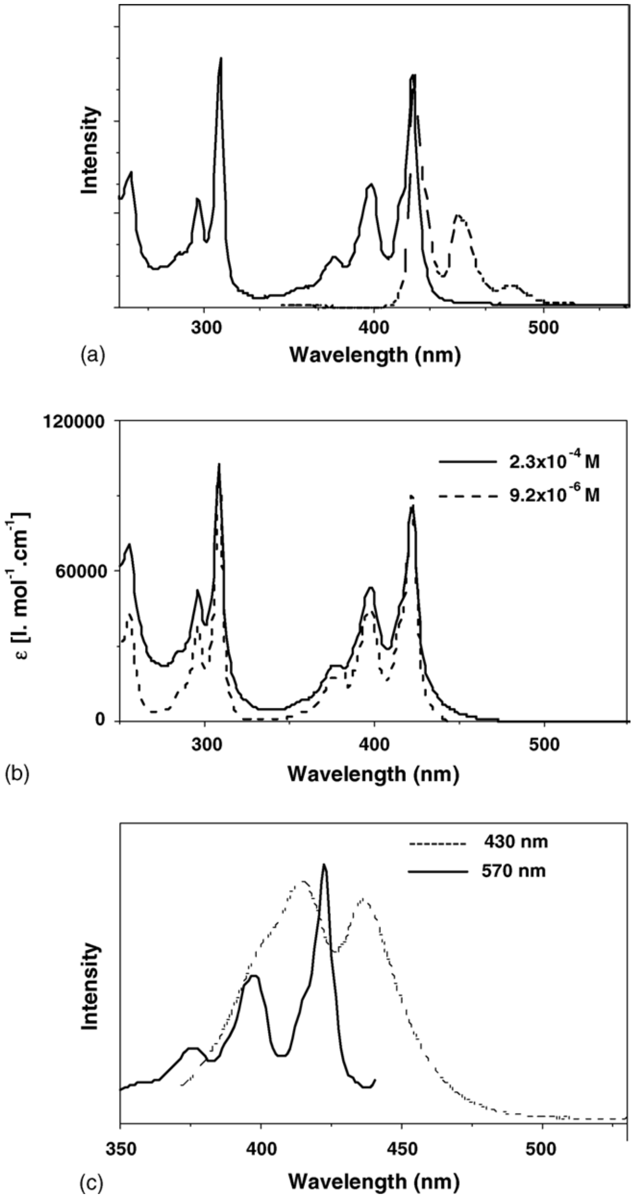

Fig. 1. (a) Normalized absorption (—) and emission (- - -) spectra of **6b** in *n*-hexane. The excitation wavelength is 310 nm. (b) Absorption spectra of **6b** in *n*-hexane at high and low concentration. (c) Normalized excitation spectra of 2.3×10^{-4} M of **6b** in *n*-hexane. The emission wavelengths are indicated in the figure.

3.4. Aggregate formation of **6b** in water

6b not only shows aggregation in apolar solvents but also in polar solvents such as water in which it is miscible. Fig. 2a

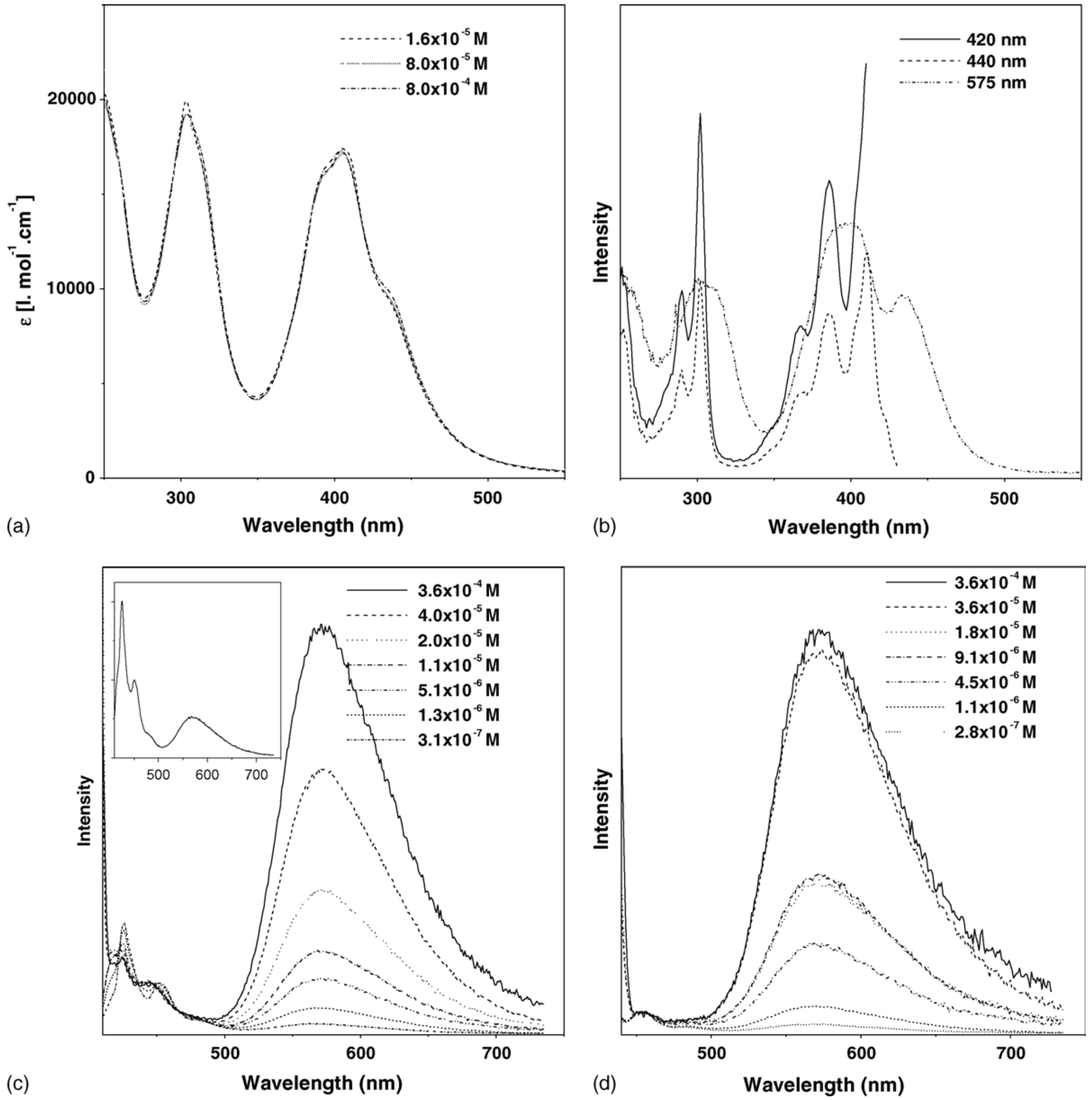

Fig. 2. (a) Concentration dependent absorption spectra of **6b** in water. (b) Emission wavelength dependent excitation spectra of a 9.1×10^{-6} M solution of **6b** in water. The emission wavelengths are indicated in the figure. (c) Normalized concentration dependent emission spectra of **6b** in water for different concentrations, as indicated in the figure, at excitation wavelengths of 400 nm and (d) 430 nm.

shows the concentration dependent optical steady-state spectra. The absorption spectra do not show a clear vibronic progression and have a significant absorption at wavelengths above 450 nm. The spectra are not concentration dependent in the concentration range studied. Fig. 2c and d shows the concentration dependent emission spectra obtained upon excitation at 400 and 430 nm, respectively.

The emission spectra are characterized by an emission band with vibronic progression in the monomer emission region and a broad unstructured band at 570 nm. The ratio of the emission band at 450 nm versus 570 nm decreases upon increasing concentration and this same ratio also decreases with increasing excitation wavelength: increasing the concentration leads to pronounced aggregate formation and the relative absorption of the aggregates versus monomer increases at increasing excitation wavelengths. The excitation spectra (Fig. 2b) recorded at an emission wavelength of 575 nm (aggregate emission) reflect the absorption spectrum, while at much shorter detection wavelengths where the monomer emission is recorded, the excitation spectrum reflects the monomer absorption. In line with aggregation, the fluorescence quantum yield is very small ($\Phi_f \sim 0.02$) which is significantly lower than that for the monomer, recorded in *n*-hexane ($\Phi_f \sim 1.00$).

These conclusions are also supported by the time-correlated single photon counting data. In contrast to the fluorescence decays collected in *n*-hexane at low concentrations, which are mono-exponential, **6b** shows multi-exponential decay behaviour in water (not shown). In agreement with the steady-state absorption and emission data, the decay traces obtained at short emission wavelengths (wavelength < 420 nm) are mono-exponential ($\tau = 2.85$ ns,) and reflect the emission of the monomer. In contrast, the decay traces obtained at longer emission wavelengths

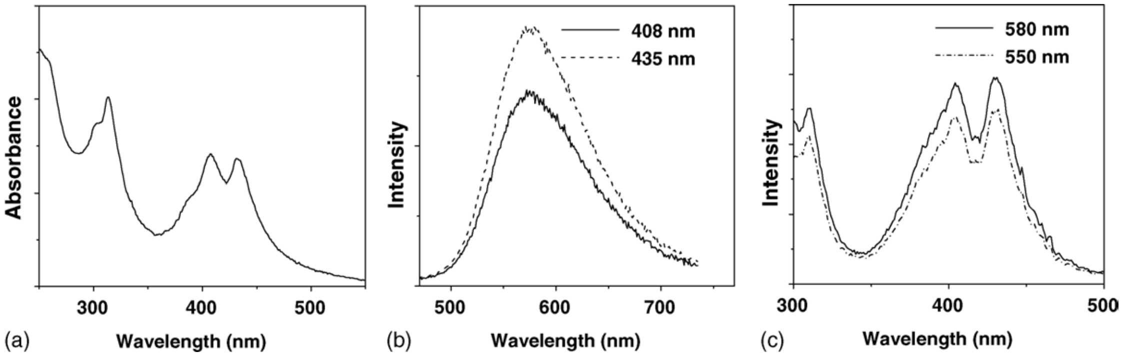

Fig. 3. (a) Absorption spectrum of **6b** drop-casted on a quartz slide. (b) Emission spectra of **6b** drop-casted on a quartz slide, $\lambda_{ex} = 408$ nm (—) and 435 nm (- - -), respectively. (c) Excitation spectra of **6b** drop-casted on a quartz slide: emission wavelengths are 580 nm (—) and 550 nm (- - -), respectively.

are multi-exponential and the relative amplitudes of the long decay components increase with increasing emission wavelengths, reflecting aggregate emission. Note that ground-state aggregates, and not diffusion-controlled excimer formation, is responsible for the long-wavelength emission.

*3.5. Aggregate formation of **6b** in neat liquid*

As mentioned, **6b** is still a liquid at room temperature. In order to investigate its spectral properties, a thin film of **6b** was prepared by drop casting from a *n*-hexane solution on a quartz plate. The spectra are presented in Fig. 3. The absorption spectrum of a film of **6b** is similar to the absorption spectrum in water. The emission band is the same as the long wavelength emission band observed for the aggregated systems discussed (vide supra). The quantum yield of fluorescence is of the order of $\Phi_f \sim 0.04$. In addition, the excitation spectrum reflects the absorption spectrum and no monomer fluorescence is observed. The time-correlated single photon counting data are multi-exponential with slowly decaying components. These data suggest that the interactions between the molecules in the aggregates formed in water and the molecules in the pure liquid are similar, since they lead to similar spectroscopic properties. The aggregation number in water has not been established, but based upon the absorption spectra, it is clear that even in the most diluted solutions, aggregates are the dominant species.

4. Conclusions

Pyrene derivatives **6b** and **6c** are liquids at room temperature whereas **6a** forms a crystalline phase with a weak cohesive energy at room temperature. Neither thermotropic nor lyotropic behaviour is observed for these compounds. Oily compounds **6b** and **6c** are miscible in solvents of polarity ranging from *n*-hexane to water. In diluted *n*-hexane solution, **6b** fluoresces quantitatively whereas in water and in neat liquid, the quantum yield of fluorescence drops to a few percents which is assigned to the presence of ground-state aggregates.

Acknowledgements

This work was financially supported by the Belgian National Science Foundation (FNRS FRFC no. 2.4560.00), by the Université Libre de Bruxelles, by the Banque National de Belgique and by the Communauté Française de Belgique (ARC no. 00/05-257). V.d.H. acknowledge the FRIA for a fellowship. The authors thank the DWTC, through IUAP-V-03 and ESF SMARTON for financial support. S.D.F. thanks the Fund for Scientific Research-Flanders for financial support.

References

[1] W. Rettig, B. Strehmel, S. Schrader (Eds.), Applied Fluorescence in Chemistry, Biology, and Medicine, Springer Verlag, Berlin, 1998.
[2] F.M. Winnik, Chem. Rev. 93 (1993) 587.
[3] (a) C.A. Backer, D.G. Whitten, J. Phys. Chem. 91 (1987) 865;
(b) N.J. Turro, P.-L. Kuo, Langmuir 3 (1987) 773;
(c) K. Kalyanasundaram, J.K. Thomas, J. Phys. Chem. 81 (1977) 23.
[4] J. Matsui, M. Mitsuishi, T. Miyashita, Macromolecules 32 (1999) 381.
[5] J. Sunamoto, H. Kondo, T. Nomura, H. Okamoto, J. Am. Chem. Soc. 102 (1980) 1146.
[6] F.D. Lewis, Y. Zhang, R.L. Letsinger, J. Org. Chem. 62 (1997) 8565.
[7] P.C. Bevilacqua, R. Kierzek, K.A. Johnson, D.H. Turner, Science 258 (1992) 1355.
[8] F. Fages, B. Bodenant, T. Weil, J. Org. Chem. 61 (1996) 3956.
[9] I. Aoki, T. Harada, T. Sakaki, Y. Kawahara, S. Shinkai, J. Chem. Soc, Chem. Commun. (1992) 1341.
[10] Y. Geerts, G. Klärner, K. Müllen, in: G. Wegner, K. Müllen (Eds.), Electronic Materials, the Oligomer Approach, VCH, Weinheim, 1998, pp. 1–103.
[11] Y. Geerts, K. Müllen, in: W. Rettig, B. Strehmel, S. Schrader (Eds.), Applied Fluorescence in Chemistry, Biology, and Medicine, Springer Verlag, 1998, pp. 299–325.
[12] J. Qu, C. Kohl, M. Pottek, K. Müllen, Angew. Chem. Int. Ed. 43 (2004) 1528.
[13] V. de Halleux, J.-P. Calbert, P. Brocorens, J. Cornil, J.-P. Declercq, J.-L. Brédas, Y. Geerts, Adv. Funct. Mater. 14 (2004) 649–659.
[14] X. Crispin, J. Cornil, R. Friedlein, V. Lemaur, A. Crispin, G. Kestemont, M. Lehmann, M. Fahlman, R. Lazzaroni, Y. Geerts, G. Wendin, J.-L. Bredas, W.R. Salaneck, J. Am. Chem. Soc. 126 (2004) 11889–11899.
[15] A. Arnaud, J. Belleney, F. Boué, L. Boutellier, G. Carrot, V. Wintgens, Angew. Chem. Int. Ed. 43 (2004) 1718.
[16] G. Jones, V. Vullev, J. Phys. Chem. A 105 (2001) 6402.
[17] D.F. Eaton, J.C. Scaiano (Eds.), Handbook of Organic Photochemistry, vol. I, CRC Press, Boca Raton, 1989, p. 231.
[18] P. Vanoppen, J. Hofkens, L. Latterini, K. Jeuris, H. Faes, J. Kerimo, P.F. Barbara, A.E. Rowan, R.J.M. Nolte, F.C. De Schryver, in: W. Rettig, B. Strehmel, S. Schrader (Eds.), Applied Fluorescence in Chemistry, Biology, and Medicine, Springer Verlag, 1998, p. 119.
[19] W. Gerhardt, R. Lehmann, WO 84/00159, 1984.
[20] H. Volmmann, H. Becker, M. Corell, H. Streeck, Justus Liebigs Ann. Chem. 531 (1937) 1–159.

[21] K. Sonogashira, Y. Tohda, N. Haghiara, Tetrahedron Lett. 50 (1975) 4467.

[22] A.G. Petrov, A. Drzhanski, Mol. Cryst. Liq. Cryst. 151 (1987) 303.

[23] A. Skoulios, D. Guillon, Mol. Cryst. Liq. Cryst. 165 (1988) 317.

[24] C. Tschierske, Annu. Rep. Prog. Chem., Sect. C 97 (2001) 1485.

[25] N. Usol’tseva, K. Praefcke, A. Smirnova, D. Blunk, Liq. Cryst. 26 (1999) 1723.

[26] D.S. Karpovich, G.J. Blanchard, J. Phys. Chem. 99 (1995) 3951.

[27] M.P. Heitz, M. Maroncelli, J. Phys. Chem. A. 101 (1997) 5852.